DOI: 10.1021/cg101012a

CRYSTAL GROWTH & DESIGN Article

2010, Vol. 10
5227–5232

Crystallographic Control of the Hydrothermal Conversion of Calcitic Sea Urchin Spine (*Paracentrotus lividus*) into Apatite

Pedro Álvarez-Lloret,*,† Alejandro. B. Rodríguez-Navarro,† Giuseppe Falini,‡ Simona Fermani,‡ and Miguel Ortega-Huertas†

†*Departamento Mineralogía y Petrología, Facultad de Ciencias, Universidad de Granada, Campus Fuentenueva, 18071 Granada, Spain, and* ‡*Dipartimento di Chimica "G. Ciamician", Alma Mater Studiorum Universitá di Bologna, via Selmi 2, 40126 Bologna, Italy*

Received August 2, 2010; Revised Manuscript Received October 20, 2010

ABSTRACT: We analyzed the crystallographic relationships during hydrothermal conversion of a calcitic sea urchin spine into apatite. We identified a pseudomorphic mineral replacement mechanism involving a superficial dissolution of calcite and a subsequent overgrowth of oriented carbonated hydroxylapatite (HA) nanocrystals. Cross-section images of these converted spines show that the dimensions of the HA crystals increase the further they are from the outer surface. This replacement process is favored by an increase in porosity, which enables both fluid and mass to be transported by diffusion, thereby allowing the replacement reaction to progress toward the interior of the spine. These recrystallization reactions take place on the surface of the calcite single crystal, which acts as a substrate for the epitaxial nucleation of HA crystals. The epitaxial relationship observed between the parent calcite crystal and the newly formed apatite crystals can be defined as (0001) apatite//(01$\bar{1}$8) calcite and [10.0] apatite//[$\bar{4}$4.1] calcite. The apatite crystals are related by the 3-fold axis arising from the trigonal symmetry of the parent calcite crystal. There is therefore a strong structural control which favors the conversion of calcite into apatite. This process coexists with the formation of apatite crystals which are not structurally related to the calcite crystal and which may precipitate within the porosity of the material. The analysis of crystallographic relationships is a fundamental step toward understanding mineral replacement reactions, which can be used for the synthesis of artificial materials with predefined shapes and microstructural characteristics, a technique that may have interesting technological applications.

1. Introduction

Mineral replacement reactions play a very important role in many natural processes and also have important technological applications. Mineral replacement occurs at a large scale in the formation of hydrothermal and metamorphic replacement formations.[1,2] In general, the presence of a reaction solution kinetically favors mineral replacement reactions. This reaction solution, acting as a fluid phase, encounters chemically reactive rocks, causing some of the mineral components to dissolve. These components are then replaced by other less soluble ones, which precipitate out of the solutions. During these replacement reactions, one mineral can be replaced by another with a different composition while preserving the external morphology and microstructural properties (e.g., porosity) of the original material, forming what is known as a pseudomorph. These mineral replacement reactions can take place by an "interface-coupled dissolution precipitation" reaction in which the dissolution rate of a parent phase is related with the precipitation of the product phase.[3,4] In particular, minerals which are highly reactive and relatively soluble, such as carbonates, react easily and are replaced by less soluble minerals, such as phosphates or silicates.[5] At a smaller scale, mineral replacement reactions in biological systems occur during the formation and maturation of calcified tissues, during which less stable precursor phases are transformed into or replaced by more stable mineral phases.[6] Previous authors have described the transformation of a parent mineral phase (e.g., amorphous calcium carbonate or amorphous calcium phosphate) into a more stable phase during the formation of biominerals such as sea urchin spines, mollusk shells, and fin bones in zebra fish.[6−8]

The pseudomorphic transformation of materials also has important technological applications, as it enables manufacturers to create a material with a predefined shape and a controlled internal microstructure by using an initial material with the appropriate shape and microstructural characteristics. An accurate control of the microstructural characteristics of a material (e.g., particle size, porosity) is critical, since these characteristics determine its physicochemical properties and its performance during its end uses.[9] Calcium carbonate materials can be converted into calcium phosphate either by hydrothermal reactions[10−13] or in reactions at ambient conditions.[14] For instance, the commercial hydroxylapatite used in bone implants is manufactured from sea corals (*Porites sp.*) that have an anatomical structure and microstructure very similar to that of human bone.[15] The original sea corals are made of calcium carbonate (aragonite) and are transformed into calcium phosphate (hydroxylapatite) using hydrothermal methods.[16,17] The resulting material preserves the microstructure and porosity of the original coral and has a composition similar to that of the bone mineral. This makes it biocompatible and suitable for use as a bone graft substitute for bone implants.[15] The same approach can be developed for the synthesis of other advanced materials, which can be produced by choosing a suitable parent material and proper experimental conditions for mineral replacement.

In this work, we have studied the crystallographic features of the hydrothermal conversion of calcium carbonate sea urchin spines into calcium phosphate. Sea urchin spines are long and rod-shaped with a very intricate porous microstructure.[18,19]

*Corresponding author. E-mail: pedalv@ugr.es.

Published on Web 11/15/2010

The spine's rounded appearance does not resemble that of a single crystal, but it diffracts as if it were one. This is very intriguing given its spongy morphology and the amount of organic matter it contains. From the crystallographic point of view, it can be described as a calcite single crystal which is elongated along the *c*-axis and has an anhedral morphology. Kasioptas et al.[11] reported the conversion of calcite single crystals into hydroxylapatite. The transformation is pseudomorphic because the external morphology of the parent calcite crystal is preserved in great detail. The formation of a very well-defined interface at the reaction front, in partially transformed crystals, may be indicative of the existence of a structural control during the transformation. Nevertheless, the crystallographic relationships between the parent calcite and the product apatite have not been previously determined. In order to determine the textural and crystallographic relationship between the parent and product phases, we have studied the material microstructure and crystallographic properties using optical, scanning and transmission electron microscopy, and X-ray diffraction techniques. In particular, to determine the three-dimensional crystallographic orientation relationship between the two phases, we have analyzed the orientation of the parent calcite crystal and the product apatite nanocrystals in partially transformed spines using X-ray diffraction texture analyses. This technique allows us to obtain pole figures containing detailed information about the orientation of the crystals that make up polycrystalline materials.[20] In this way, it is possible to determine the crystallographic orientations of the parent and product phases and define the structural relationship between them. Furthermore, the microscopy and diffraction techniques used here are complementary, as they provide information about the textural organization of the material at different scales, from the millimeter (optical microscopy, XRD texture analyses) to the nanometer scale (TEM). This information can give us important insights into the mechanism(s) controlling the transformation between these mineral phases, in particular, if the transformation mechanism is controlled by structural factors (e.g., epitaxy). From the point of view of material science, a study of the mechanisms/processes taking place during the transformation of minerals can provide valuable information to enable us to synthesize artificial materials with specific technological and industrial applications.[21] Understanding the precipitation and transformation mechanisms of carbonate and phosphate minerals is of great importance, since these minerals control the chemistry of aqueous systems and are also the main components of mineralized tissues in vertebrate skeletons such as bone and teeth (made of calcium phosphate) or invertebrate exoskeletons such as mollusc shells (made of calcium carbonate).

2. Materials and Experimental Methods

2.1. Biogenic Calcite Conversion to Hydroxyapatite. Spines were collected from different specimens of *Paracentrotus lividus* sea urchins. The spines were treated with 2.5% (v/v) NaClO solution for 24 h to remove extraskeletal organic matter. They were washed in milli-Q water and finally dried at 60 °C for 2 h. Samples about 10 mm in length were selected for hydrothermal conversion into HA. Various reaction conditions were tested. The optimal experimental set up was found to be the following: five spines were put in a 100 mL Teflon vessel together with 50 mL of 300 mM sodium phosphate solution, pH 7.4. The hydrothermal reaction was carried out for 24 h in a Parr reactor 4564 at 180 °C on the saturated vapor pressure curve. After the reaction the spines were carefully washed with deionized water several times and then dried in the oven at 60 °C.

2.2. Characterization of Sea Urchin *P. lividus* Spine Samples. 2.2.1. Density and Porosity. Measurements were carried out on four samples of HA converted spines and on four samples of parent spines. The buoyant method, initially developed for corals, was used because it is simple and nondestructive.[22] Initially the spines were put in a desiccator connected to a pump (10^{-2} atm) for about 4 h in order to drive out all the air from the exposed pores. Still under vacuum conditions, the spines were then soaked by gradually pouring water into the desiccator.[23] The weight was measured using an Ohaus Explored Pro balance. The standard pan was replaced with a suspended weighing cradle attached to an underwater weighing pan submerged in a glass beaker filled with distilled water. A cover isolated the mechanism from air turbulence within the laboratory. To calculate the buoyant weight, the spine was slowly lowered onto the underwater weighing pan (making sure that no air bubbles adhered to its surface). The buoyant weight measurement was taken 5 s after placing the spine in the pan. To obtain the weight of the spine, in which the exposed pores were water-filled, it was taken out of the water, quickly blotted with a moist paper towel, and reweighed in air. The density and the porosity were also obtained from the above measurements

2.2.2. Imaging. Optical microscopy observations were carried out using a SX40 Olympus petrographic microscope equipped with a CCD camera. Scanning electron microscopy (SEM) images were collected on samples that were glued onto an aluminum stub after being coated with gold and observed with a Philips 515 scanning electron microscope. The observations were carried out at a voltage of 20 kV. Transmission electron microscopy (TEM) observations on spines were carried out using a STEM PHILIPS CM20 transmission electron microscope operated at an acceleration voltage of 80 kV. Samples of *P. lividus* spines were embedded in resin and cut into thin sections (~200 nm thickness) for TEM observations using an ultramicrotome.

2.2.3. X-ray Diffraction. Two-dimensional X-ray diffraction and pole figures describing the three-dimensional orientation of the calcite and apatite phases in partially converted sea urchin spines were determined using an X-ray single crystal diffractometer equipped with a CCD area detector (D8 SMART APEX, Bruker, Germany). For diffraction experiments, the working conditions were as follows: Mo Kα (λ = 0.7093 Å), 50 kV, and 30 mA, a pinhole collimator of 0.5 mm in diameter, and an exposure time of 20 s per frame. Converted sea urchin spines were analyzed by reflection mode (diffractometer ω and 2θ angles were set at 10 and 20°, respectively). A set of 2D diffraction patterns were registered while rotating the sample around the Φ angle (a frame was registered every 5°). Pole densities/figures for the main calcite and apatite reflections were calculated from the frames registered using XRD2DScan software.[24] These pole figures represent the intensity variation of a particular *hkl* reflection as a function of the sample orientation.

3. Results

Biogenic calcite single crystals containing magnesium ions were converted into calcium phosphates, thus producing carbonated hydroxylapatite in which there may be a small amount of foreign ions (sodium and magnesium). In the following sections, based on X-ray diffraction and FTIR data, we refer to this nonstoichiometric crystalline material as carbonated hydroxylapatite (HA).

This hydrothermal conversion was accompanied by changes in both the porosity and the density of the material, results which were determined as described above in the Experimental Section. The porosity increased from 21(2)% to 29(3)%, while the density changed from 2.64(8) mg/cm^3 to 2.9(1) mg/cm^3.

Optical microscopy examination of the converted sea urchin spines revealed that their external morphology had been preserved with a high degree of fidelity, which indicates that the transformation is pseudomorphic. Futhermore, cross sections of the spines showed that their intricate inner porous structure had also been preserved (Figure 1a−c). Inspection of the sea urchin spines at higher magnification (TEM analyses) revealed that the original calcite crystal had been replaced by

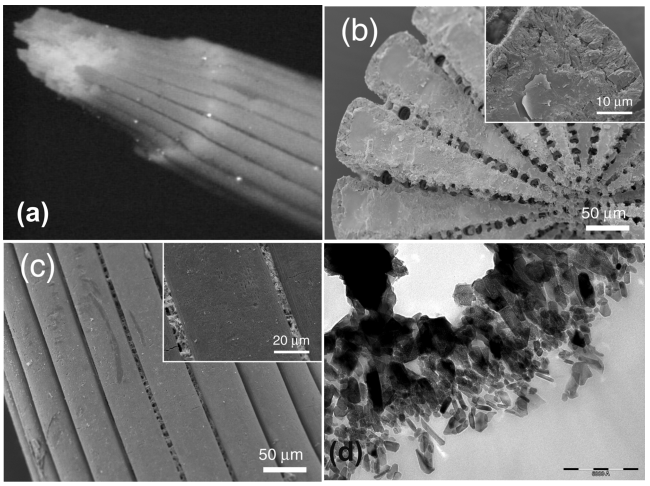

Figure 1. (a) Photograph of a transformed sea urchin spine showing the external shape and porosity of the original material. (b) SEM image of the cross section of a spine showing the well-preserved internal microstructure and its complex spongy morphology. (c) SEM image of the external morphology of the original calcitic sea urchin spine. (d) TEM image of converted sea urchin spines showing the newly formed apatite crystals, which are elongated and increase in size from the outer surface inward.

nanosized apatite crystals with an elongated rodlike morphology (Figure 1d). We also observed that the size of the apatite crystals increased the further away they were from the outer surface and that there was a significant increase in the porosity of the material due to the space left between the apatite crystals.

In addition, bidimensional X-ray diffraction patterns of partially converted sea urchin spines show the presence of strong single crystal diffraction spots from the parent calcite crystal and several diffraction rings of the product apatite crystals (Figure 2a). The diffraction rings have a continuous intensity and are associated with randomly oriented apatite crystals (Figure 2b). Superimposed on these rings, the intensity is concentrated in arcs, which indicates that a small fraction of the apatite crystals have a strong preferential orientation. Thus, the 2D-XRD data reveal that there are two coexisting populations of apatite crystals, one made up of randomly oriented crystals that accounts for about 80% of the total and the other made up of co-oriented crystals that accounts for the remaining 20%. The percentage of each population has been estimated by measuring the contribution of each fraction to the total intensity of several Debye−Scherrer rings of apatite crystals. The random fraction contributes with a ring of continuous intensity and the oriented fraction with an arc produced by co-oriented crystals reflecting on the same portion of the ring. This enables the intensity of each fraction to be measured separately.

The preferential orientation of the apatite crystals in relation to the parent calcite single crystal was further characterized by the determination of pole figures for the main reflections of both mineral phases. Thus, in order to define the orientation of the parent calcite crystal, we had to determine the pole figures for the 006, 110, and 104 reflections of apatite crystals, whereas the pole figures for reflections 002, 004, 121, 020, and 010 were required for defining the orientation of the product apatite crystals. The pole figures for calcite reflections 006, 110 (not shown), and 104 indicate that the spine is made up of a single crystal of calcite with the *c*-axis oriented parallel to the elongation axis of the spine (Figure 3a and b), whereas

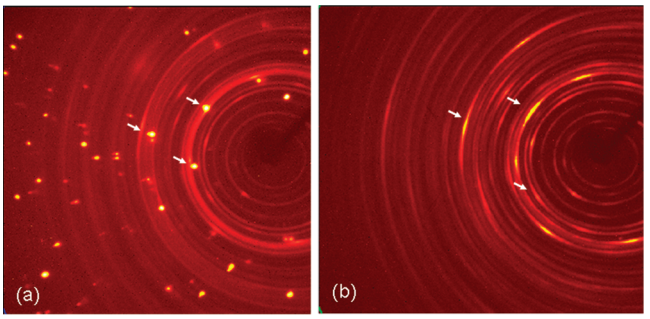

Figure 2. Bidimensional X-ray diffraction (2DRXD) patterns from sea urchin spines with different degrees of hydrothermal conversion. (a) Partially converted spine showing the presence of the original calcite (as strong single crystal spots; see arrows) and apatite crystals (Debye−Scherrer rings). (b) Fully converted spine showing continuous diffraction rings associated with randomly oriented apatite crystals. Superimposed on the diffraction rings, the intensity is concentrated in arcs (see arrows), indicating that a small fraction of apatite crystals have a strong preferential orientation.

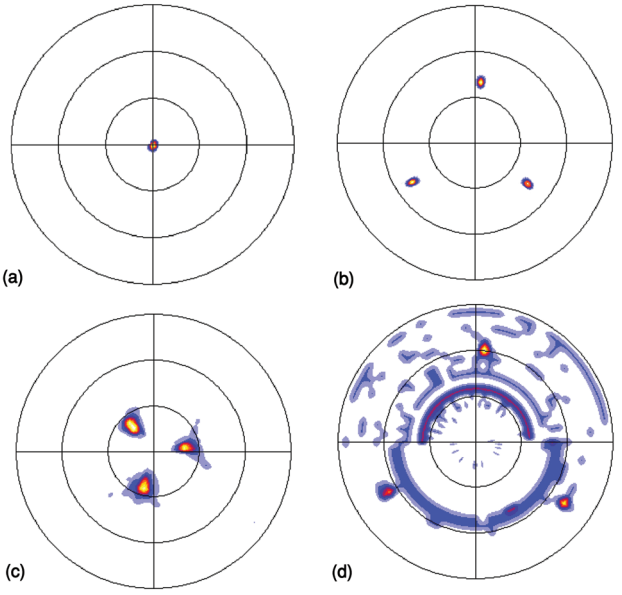

Figure 3. Pole figures from partially converted sea urchin spines showing the crystallographic orientation relationship between the parent calcite crystal and the product apatite crystals. (a) 006 pole figure for calcite showing a maximum at the center, indicating that the calcite *c*-axis is parallel to the spine elongation axis. (b) 104 pole figure for calcite displaying three well-defined maxima tilted 44° and rotated around the *c*-axis 120° according to the 3-fold symmetry of calcite. (c) 002 pole figure for apatite crystals displaying three maxima tilted about 26° and rotated 120° around the *c*-axis of the parent calcite. (d) 010 pole figure for apatite crystals displaying three maxima tilted at about 65° and rotated around 120°.

pole figures for the 002 and 004 (not shown) reflections of apatite crystals indicate that there are three sets of crystals with different crystallographic orientations (Figure 3 c). Each set of apatite crystals is oriented with their *c*-axis tilted about 26° from the *c*-axis of the parent calcite and rotated 120° around the original calcite *c*-axis. Therefore, the three sets of apatite crystals are arranged according to the 3-fold symmetry of the parent calcite crystal. Moreover, the pole figure for the 010 reflection of apatite crystals (Figure 3 d) displays three well-defined maxima placed at a coincident angular position from the maxima positions of the 104 reflections of calcite

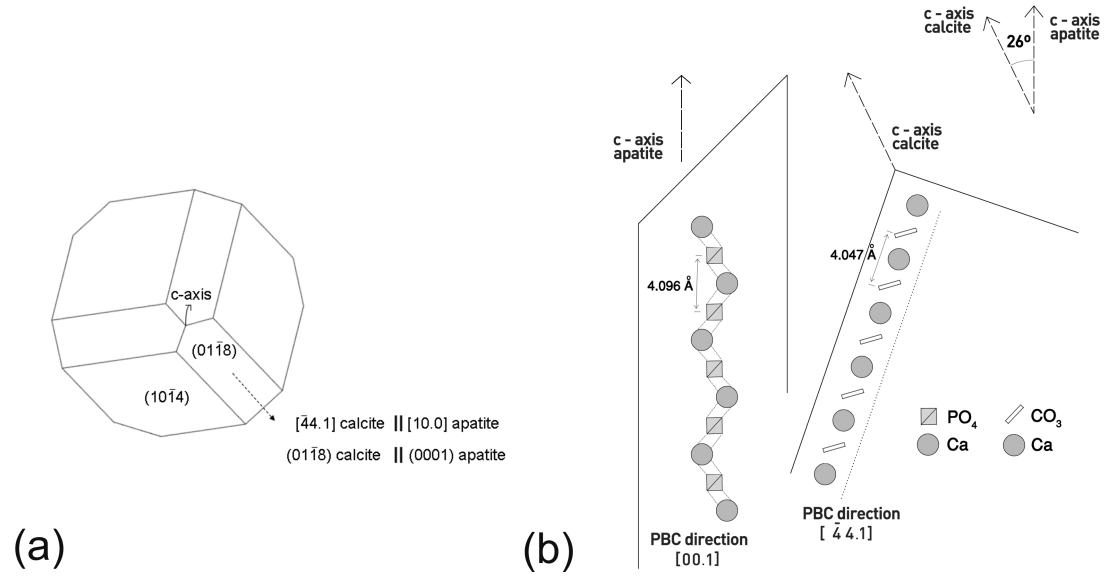

Figure 4. Model for epitaxial relationship between calcite and apatite phases. (a) Apatite crystals nucleate epitaxially with their {0001} planes on {01$\bar{1}$8} calcite surfaces, so that apatite *c*-axes are perpendicular to these crystallographic planes. (b) This epitaxial relationship is mainly determined by the correspondence between the periodic bond chains running along [00.1] in apatite and [$\bar{4}$4.1] in calcite, which have the same distance between phosphate and carbonate groups, respectively. The three sets of apatite crystals are related by 3-fold symmetry of the parent calcite crystal.

crystal (Figure 3 b). Thus, this crystallographic relationship is indicative of a structurally controlled conversion in which there are three sets of apatite crystals arranged according to the 3-fold symmetry of the parent calcite crystal. This specific arrangement is produced by an epitaxial nucleation of apatite on calcite surfaces. The epitaxial relationship between calcite and apatite crystals can be expressed as follows: (0001) apatite //(01$\bar{1}$8) calcite and [10.0] apatite//[$\bar{4}$4.1] calcite (Figure 4).

4. Discussion

The reaction of calcitic sea urchin spines with a solution of sodium phosphate produces a pseudomorph made of hydroxylapatite which accurately reproduces the complex external and internal morphology of the original sea urchin spine. The calcite single crystal that forms the original spine is replaced by nanosized elongated apatite nanocrystals growing out of the original external surface. This process is associated with an increase in porosity and a change in density from 2.6 mg/cm^3 to 2.9 mg/cm^3, which is lower than the density for apatite, 3.2 mg/cm^3. The increase in porosity, from 21% to 29%, could be associated with the proposed mechanism of conversion. A minor contribution to this increase could also come from the release of organic macromolecules from the original biogenic calcite crystals.

Previous authors have reported the hydrothermal conversion of calcite crystals into a polycrystalline apatite pseudomorph.[10] They proposed that the mineral replacement reaction takes place by an interface coupled dissolution/recrystallization mechanism and that there was a strong structural control on the transformation from calcite to apatite phases. The epitaxial growth of hydroxylapatite on calcite crystals is due to the fact that they have similar crystal structures: e.g. similar symmetry and unit cell dimensions. In particular, these authors described the following epitaxial relationships: (0001)calcite// (0001)apatite or (10$\bar{1}$0)calcite//(10$\bar{1}$0)apatite.[25,26] In this study we found that there is an oriented nucleation of apatite crystals on calcite crystals which can be described by the following hitherto unreported epitaxial relationship: (0001) apatite//(01$\bar{1}$8) calcite and [10.0] apatite//[$\bar{4}$4.1] calcite. This relationship is the result of the fact that there are similar distances between carbonate groups and phosphate groups in the periodic bond chains (PBCs) running along the matching crystallographic directions in both crystal structures. The distances between adjacent phosphates and carbonates groups along these directions are 4.096 Å and 4.047 Å, respectively (distances obtained from ref 27). PBCs are privileged directions within the crystal structure which contain an uninterrupted chain of ions connected by strong bonds. These directions control the growth and morphology of a crystal.[28] In any case, this relationship indicates that the mineral replacement must occur at the solution/calcite interface by an epitaxial nucleation of apatite crystals on the surface of dissolving calcite crystals, so that the orientation of the parent calcite determines the disposition of apatite nanocrystals. At this interface, CO_3^{2-} ions must be replaced by PO_4^{3-} in such a way that the structure of the original calcite is partially preserved on the surface on which apatite crystals nucleate epitaxially. These results confirm those of other studies in which the pseudomorphic transformation is generally determined by a crystallographic control due to a match between the parent and product crystal structures, which could be either epitactic or topotactic.[2,29] A similar epitaxial growth mechanism between brushite and gypsum has previously been described in both natural and synthetic systems.[30,31] In previous works, Yanagisawa et al.[32] also reported an experimental replacement by hydrothermal conversion in which chlorapatite was transformed into hydroxylapatite through a cation exchange mechanism preserving the crystallographic orientation of the parent phase. In all cases, the structural relationship can lower the supersaturation conditions needed for the nucleation of the new mineral phase on the interface of the parent mineral phase, as compared to the conditions required for the precipitation of the same minerals out of a free solution.[33]

We also observed a second population of apatite crystals which had no orientation relationship with the parent calcite crystal. This population of randomly oriented apatite crystals

must be the result of a nonordered replacement of the carbonate material with no structural control, for instance, by the precipitation of apatite crystals out of the solution, which are then trapped inside the porosity created by the dissolution of the parent calcitic spine or by the transformation from a precursor amorphous phase (e.g., ACP or OCP), which would not establish any predefined orientation for the product phase.

The relative solubility of minerals and porosity generation are also important factors in determining the pseudomorphic transformation of minerals. As regards the first factor, the sodium phosphate solution in which the calcitic spine is soaked is undersaturated with respect to calcite, which makes it dissolve, so releasing Ca and CO_3 ions to the carbonate interface. However, at this interface, when the solution becomes supersaturated with respect to apatite (which is far less soluble than calcite), apatite crystals can start to precipitate and replace the original material. Furthermore, during calcite to apatite conversion, there is a reduction in molar volume[11] which increases the porosity level. This porosity provides pathways for mass transport, allowing the replacement reaction to progress toward the inside of the material. Volume changes during transformation of mineral phases either slow down or accelerate reaction rates, as they increase or reduce the permeability of the interface.

The principal conclusions of this study are as follows: (1) the mineral replacement of the biogenic calcite single crystal by the assembly of hydroxyapatite crystals is pseudomorphic, as all fine morphological details and macroscale porosity of the original material are preserved; (2) the polycrystalline apatite replacing material is made up of two populations of apatite crystals, one formed by randomly oriented apatite crystals and the other by preferentially oriented apatite crystals; (3) there are three sets of apatite crystals related by a 3-fold axis [This arrangement is inherited from the calcite crystal by the epitaxial nucleation of apatite crystals on three symmetrically related {01−18} calcite surfaces.]; (4) there is a volume reduction resulting in the generation of new porosity between apatite crystals which allows fluid infiltration toward the replacement reaction front; (5) this mineral replacement reaction may be explained as a dissolution/recrystallization reaction enhanced by the diffusion of ions through the fluid phase and by the epitaxy existing between the parent and product phases.

It has been shown that the parent calcite crystal has a crystallographic control over the precipitated phase of the apatite. In this way, the calcite crystal from the biogenic *P. lividus* spine plays a fundamental role by acting as a template on which to obtain a complex assembly of oriented apatite crystals, which are arranged according to the 3-fold symmetry of the parent calcite crystal. This is explained by the epitaxial relationship between calcite and apatite crystal structures described above. The transformation reaction is therefore largely controlled by this structural relationship. However, we cannot rule out the possibility that the occluded organic matrix or the magnesium in the Mg-calcite spine plays a role in this mineral transformation mechanism. It would be useful to identify whether specific molecular interactions exist at inorganic−organic interfaces that can control the nucleation and growth of the newly formed HA inorganic crystals. This study also shows that it is possible to manufacture materials made of HA with very complex shapes and internal microstructures by means of conversion from starting materials such as a sea urchin spine. HA crystals are deposited on the biogenic calcite single crystals from a sodium phosphate solution. In this process, the biogenic calcite crystal plays a double role as the source of calcium ions and as a template to obtain an oriented assembly of HA crystals. This study could be useful when devising new strategies in the controlled synthesis of biomimetic inorganic nanophases, leading to the development of organized biocomposites and ceramic materials. These transformed HA materials have a promising future as orthopedic and dental implants with enhanced biological and biomechanical properties. Also, the increase in the surface area may improve the biocompatibility of the material. The biomimetic assemblies can potentially be used as small bone implants (e.g., as bone scaffolds[34] or as nails for the fixation of bone fractures) or in other technological applications in which an accurate control of the morphology and the microstructure (porosity) characteristics are important (e.g., controlled drug release).[35]

Acknowledgment. This work was supported by Project P08-RNM4169 and Research Group RNM-179 (Junta de Andalucía, Spain). We thank M. M. Abad-Ortega and J. Romero-Garzón (Centro de Instrumentación Científica, Universidad de Granada) for their technical assistance during HREM and XRD analyses. We also thank Dr. Luca Pasquini of the Department of Physics of the University of Bologna for the density and porosity measurements. G.F. and S.F. thank the Consorzio Interunivesitario di Ricerca della Chimica dei Metalli nei Sistemi Biologici for its financial support. We would also like to thank three anonymous reviewers for their useful comments and corrections.

References

(1) Nesse, W. D. *Introduction to Mineralogy*; Oxford University Press: New York, Oxford, 2000; +442 pp.
(2) Putnis, A. *Rev. Mineral. Geochem.* **2009**, *70*, 87–124.
(3) Kasioptas, A.; Geisler, T.; Putnis, C. V.; Perdikouri, C.; Putnis, A. *J. Cryst. Growth* **2010**, *312*, 2431–2440.
(4) Xia, F.; Brugger, J.; Ngothai, Y.; O'Neill, B.; Chen, G.; Pring, A. *Cryst. Growth Des.* **2009**, *9*, 4902–4906.
(5) Ames, J. R. L. L. *Econ. Geol.* **1959**, *54*, 829–841.
(6) Addadi, L.; Raz, S.; Weiner, S. *Adv. Mater.* **2003**, *15*, 959–970.
(7) Mahamid, J.; Sharir, A.; Addadi, L.; Weiner, S. *Proc. Natl. Acad. Sci. U.S.A.* **2008**, *105*, 12748–12753.
(8) Politi, Y.; Arad, T.; Klein, E.; Weiner, S.; Addadi, L. *Science* **2004**, *306*, 1161–1164.
(9) Kocks, U. F.; Tome, C. N.; Wenk, H. R. *Texture and Anisotropy. Preferred Orientations in Polycrystals and their Effect on Materials Properties*; Cambridge University Press: Cambridge, U.K., 2001.
(10) Ni, M.; Ratner, B. D. *Biomaterials* **2003**, *24*, 4323–4331.
(11) Kasioptas, A.; Perdikouri, C.; Putnis, C. V.; Putnis, A. *Mineral. Mag.* **2008**, *72*, 77–80.
(12) Rocha, J. H. G.; Lemos, A. F.; Agathopoulos, S.; Kannan, S.; Valério, P.; Ferreira, J. M. F. *J. Biomed. Mater. Res., A* **2006**, *77*, 160–168.
(13) Vecchio, K. S.; Zhang, X.; Massie, J.; Wang, M.; Kim, C. *Acta Biomater.* **2007**, *3*, 785–793.
(14) Marchegiani, F.; Cibej, E.; Vergni, P.; Tosi, G.; Fermani, S.; Falini, G. *J. Cryst. Growth* **2009**, *311*, 4219–4225.
(15) Damien, E.; Revell, P. A. *J. Appl. Biomater. Biomech.* **2004**, *2*, 65–73.
(16) Roy, D. M.; Linnehan, S. A. *Nature* **1974**, *247*, 220–227.
(17) Jinawath, S.; Polchai, D.; Yoshimura *Mater. Sci. Eng., C* **2002**, *22*, 35–39.
(18) Berman, A.; Addadi, L.; Kvick, A.; Leiserowitz, L.; Nelson, M.; Weiner, S. *Science* **1990**, *250*, 664–667.
(19) Moureaux, C.; Pérez-Huerta, A.; Compère, P.; Zhu, W.; Leloup, T.; Cusack, M.; Dubois, P. *J. Struct. Biol.* **2010**, *170*, 41–49.
(20) Rodríguez-Navarro, A. B.; CabraldeMelo, C.; Batista, N.; Morimoto, N.; Alvarez-Lloret, P.; Ortega-Huertas, M.; Fuenzalida, V. M.; Aria, J. I.; Wiff, J. P.; Arias, J. L. *J. Struct. Biol.* **2006**, *156*, 355–362.
(21) Meyers, M. A.; Chen, P.-Y.; Lin, A. Y.-M.; Seki, Y. *Prog. Mater. Sci.* **2008**, *53*, 1–206.
(22) Bucher, D. J.; Harriott, V. J.; Roberts, L. G. *J. Exp. Mar. Biol. Ecol.* **1998**, *228*, 117–136.

(23) Barnes, D. J.; Devereux, M. J. *J. Exp. Mar. Biol. Ecol.* **1988**, *121*, 37–54.
(24) Rodriguez-Navarro, A. B. *J. Appl. Crystallogr.* **2006**, *39*, 905–909.
(25) Lonsdale, K. *Nature* **1968**, *217*, 56–58.
(26) Koutsoukos, P. G.; Nancollas, G. H. J. *J. Cryst. Growth* **1981**, 10–19.
(27) Wyckoff, R. W. G. *Crystal Structures*; John Wiley & Sons: New York, London, 1964; Vol. 2.
(28) Hartman, P. *Crystal growth: an introduction*; North-Holland/American Elsevier: Amsterdam, London. 1973.
(29) Putnis, A. *Introduction to Mineral Sciences*; Cambridge University Press: Cambridge, New York, Port Chester, Melbourne, Sydney, 1992; +457 pp.
(30) Abbona, F.; Christensson, F.; Angela, M. F.; Madsen, H. E. L. *J. Cryst. Growth* **1993**, *131*, 331–346.
(31) Pinto, A. J.; Jimenez, A.; Prieto, M. *Am. Mineral.* **2009**, *94*, 313–322.
(32) Yanagisawa, K.; Rendon-Angeles, J. C.; Ishizawa, N.; Oishi, S. *Am. Mineral.* **1999**, *84*, 1861–1869.
(33) Putnis, A.; Putnis, C. V. *J. Solid State Chem.* **2007**, *180*, 1783–1786.
(34) Wang, M. *Ceram. Trans.* **2010**, *218*, 175–183.
(35) Al-Kattan, A.; Errassifi, F.; Sautereau, A.-M.; Sarda, S.; Dufour, P.; Barroug, A.; Santos, I. D.; Combes, C.; Grossin, D.; Rey, C.; Drouet, C. *Adv. Eng. Mater.* **2010**, *12*, B224–B233.